

1º Simpósio NOVACAP

A tecnologia nas coberturas das arenas de 2014

Tensoestruturas: ideias básicas e algumas aplicações aos projetos de estádios

Ruy Marcelo de Oliveira Pauletti

Escola Politécnica da Universidade de São Paulo



Brasília, 04/12/2012

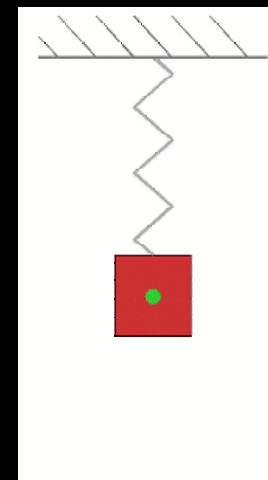


Taut Structures:

“those that require their elements to be **taut**, instead of **slack** or **wrinkled**, to work properly.

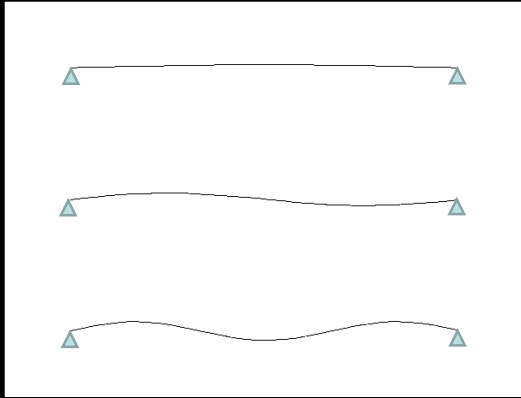


A spring-mass system:



$$f = \frac{1}{2\pi} \sqrt{\frac{k}{m}}$$

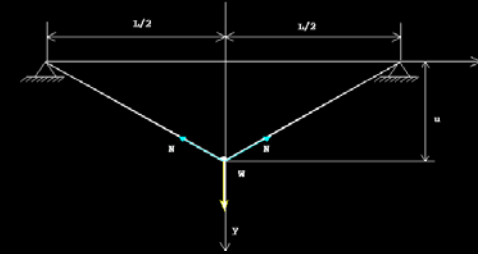
A vibrating string:



$$f = n\pi \sqrt{\frac{T}{mL}}$$

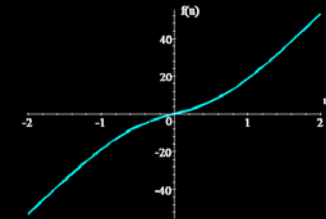
$$k_g \sim \frac{T}{L}$$

A transversely loaded string:



$$k = \frac{EA}{\ell_r} \quad \ell_r < L$$

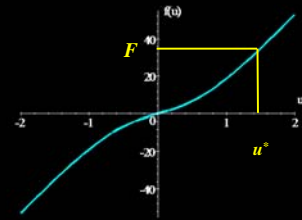
$$P(u) = 4k \left(1 - \frac{\ell_r}{\sqrt{L^2 + 4u^2}} \right) u$$



Non-linear equilibrium:

Given F , find u^* such that

$$g(u^*) = P(u^*) - F = 0$$

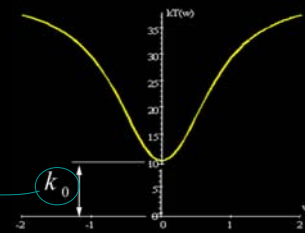


Newton's Method:

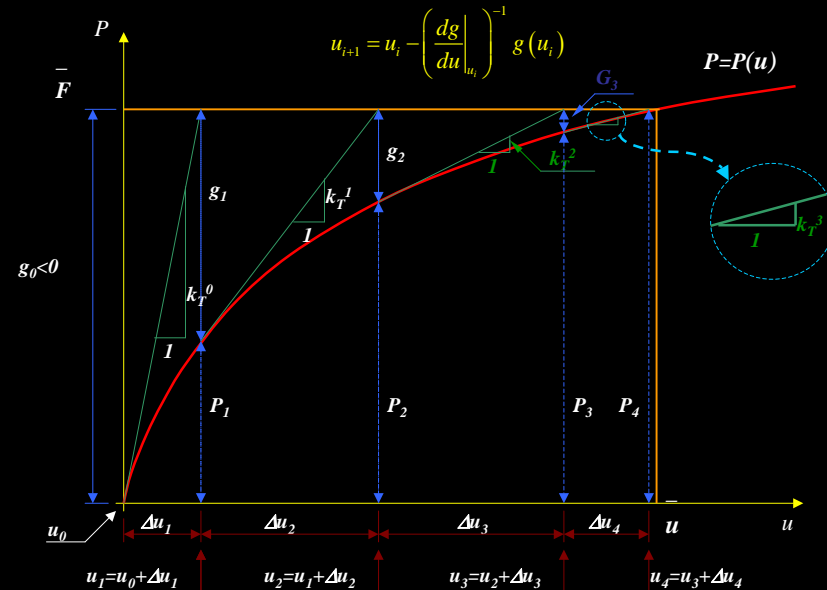
$$u_{i+1} = u_i - \left(\frac{dg}{du} \Big|_{u_i} \right)^{-1} g(u_i)$$

Tangent stiffness $k_{t_i} = \frac{dg}{du} \Big|_{u_i}$

$$k_0 = \frac{4T_0}{L}$$



Newton's Method for a scalar problem $g=P(u)-F=0$



Geometrically Non-Linear Equilibrium, for many DOF:

$$\text{Find } \mathbf{u}^* \text{ such that } \mathbf{g}(\mathbf{u}^*) = \mathbf{P}(\mathbf{u}^*) - \mathbf{F}(\mathbf{u}^*) = \mathbf{0}$$

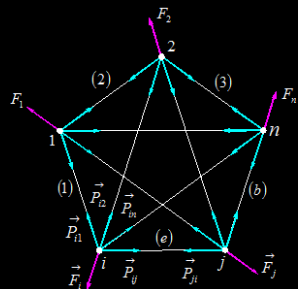
- $\mathbf{P} = \mathbf{P}(\mathbf{u})$ Internal Load Vector
- $\mathbf{F} = \mathbf{F}(\mathbf{u})$ External Load Vector
- $\mathbf{g} = \mathbf{g}(\mathbf{u})$ Unbalanced ('Error') Load Vector

Newton's method for many DOFs:

$$\mathbf{u}_{i+1} = \mathbf{u}_i - \left(\frac{\partial \mathbf{g}}{\partial \mathbf{u}} \bigg|_{\mathbf{u}_i} \right)^{-1} \mathbf{g}(\mathbf{u}_i) = \mathbf{u}_i - \left(\mathbf{K}_t^i \right)^{-1} \mathbf{g}(\mathbf{u}_i)$$

$$\mathbf{K}_t^i = \frac{\partial \mathbf{g}}{\partial \mathbf{u}} \bigg|_{\mathbf{u}_i} \quad \text{Tangent stiffness matrix}$$

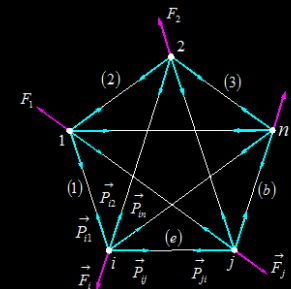
A System of Central Forces



$$\mathbf{F} = \begin{bmatrix} \mathbf{f}_1 \\ \mathbf{f}_2 \\ \vdots \\ \mathbf{f}_n \end{bmatrix}; \quad \mathbf{P} = \begin{bmatrix} \mathbf{p}_1 \\ \mathbf{p}_2 \\ \vdots \\ \mathbf{p}_n \end{bmatrix}$$

$$\mathbf{p}_i = \sum_{j=1}^n \mathbf{p}_{ij} = \sum_{j=1}^n N_{ij} \mathbf{v}_{ij} = \sum_{j=1}^n N_{ij} \frac{\mathbf{x}_j - \mathbf{x}_i}{\|\mathbf{x}_j - \mathbf{x}_i\|}, \quad i=1, \dots, n$$

A System of Central Forces



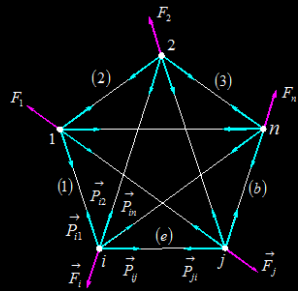
$$\mathbf{P} = \mathbf{CN}$$

"Geometric operator"

Vector of internal element loads

$$\mathbf{C} = \sum_{(e)=1}^b \mathbf{C}^{(e)} = \sum_{(e)=1}^b \begin{bmatrix} 1 & \dots & (e) & \dots & b \\ 0 & \dots & 0 & \dots & 0 \\ 0 & \dots & -\mathbf{v}^{(e)} & \dots & 0 \\ \vdots & \vdots & \vdots & \vdots & \vdots \\ 0 & 0 & \mathbf{v}^{(e)} & 0 & 0 \\ \vdots & \vdots & \vdots & \vdots & \vdots \\ n & 0 & 0 & \dots & 0 \end{bmatrix}_{b \times b} \quad \mathbf{N} = \begin{bmatrix} N_1 \\ N_2 \\ \vdots \\ N_b \end{bmatrix}_{b \times 1}$$

A System of Central Forces



$$\mathbf{P} = \mathbf{CN}$$

"Geometric operator"

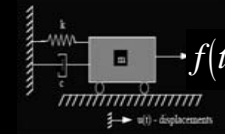
Vector of internal element loads

$$\mathbf{K}_t = \frac{\partial}{\partial \mathbf{u}} (\mathbf{CN} - \mathbf{F}) = \mathbf{C} \frac{\partial \mathbf{N}}{\partial \mathbf{u}} + \mathbf{N}^T \frac{\partial \mathbf{C}}{\partial \mathbf{u}} - \frac{\partial \mathbf{F}}{\partial \mathbf{u}}$$

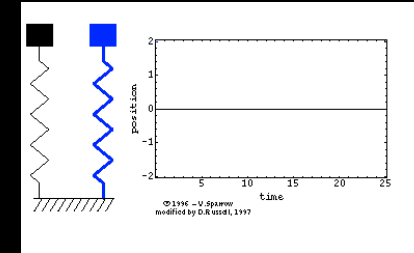
$$\mathbf{K}_t = \mathbf{K}_c + \mathbf{K}_g + \mathbf{K}_{ext}$$

The Dynamic Relaxation Method

A single DOF oscillator:

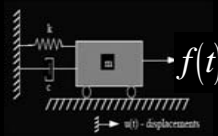


$$m\ddot{u} + c\dot{u} + p(u) = f(t)$$



The Dynamic Relaxation Method

A single DOF oscillator:



$$m\ddot{u} + c\dot{u} + p(u) = f(t)$$

A linear SDOF oscillator under a step force:

$$p(u) = ku$$

$$f(t) = \begin{cases} 0, & t < 0 \\ F, & t \geq 0 \end{cases}$$

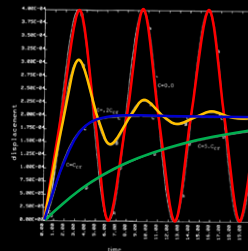
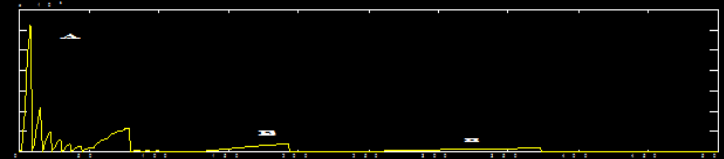


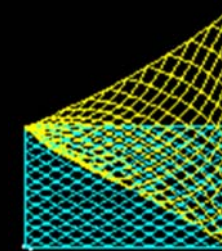
Figure 28.1 Displacement versus time curves with a variety of damping coefficients applied to a one degree of freedom oscillator.

The Dynamic Relaxation Method

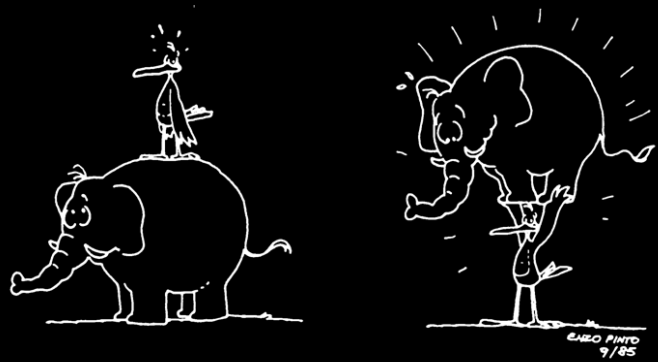
Kinetic Damping:



Transient of kinetic energy during the shape finding of a cable network via DR, with kinetic damping

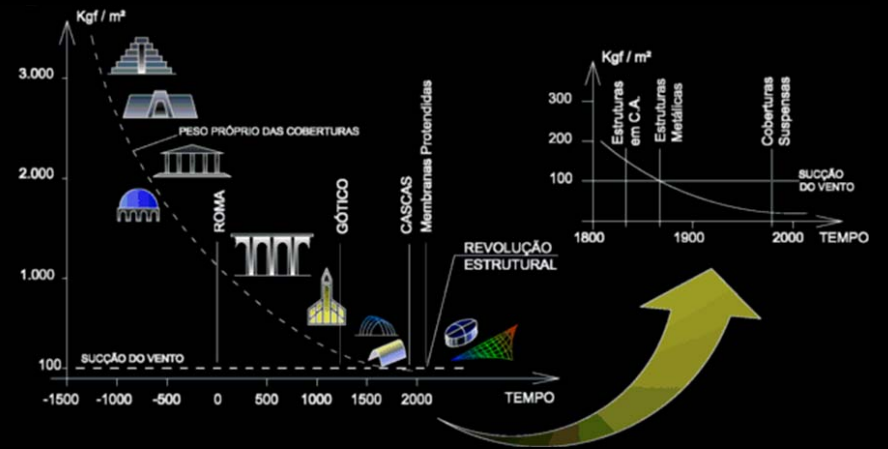


“Light structures”



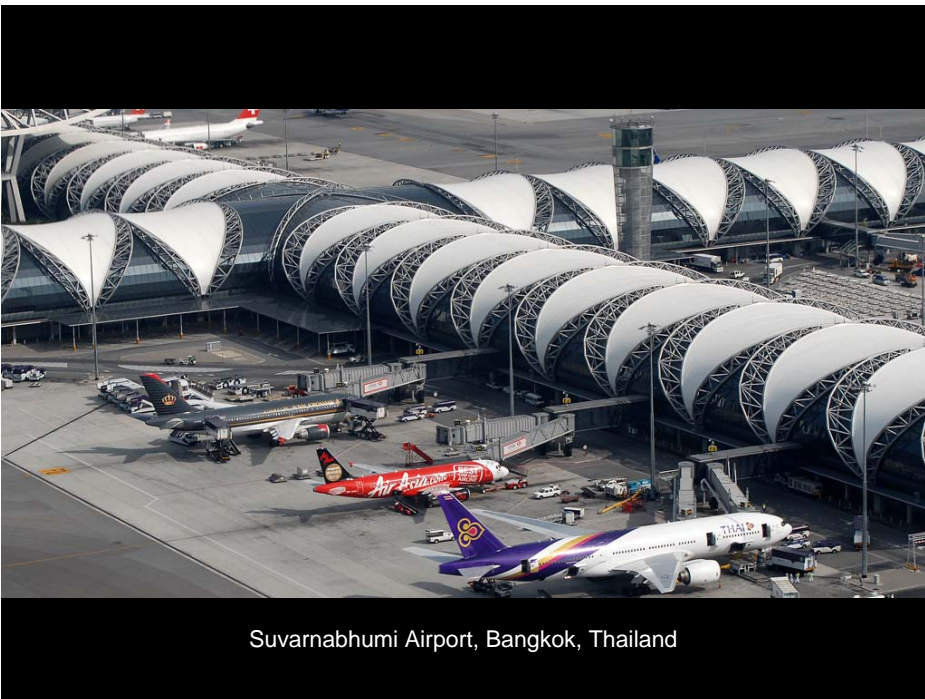
“Peso portante << Peso portado”
(Majowiecki, 1994)

“Light structures”



“Light structures, structures of light” – H. Berger



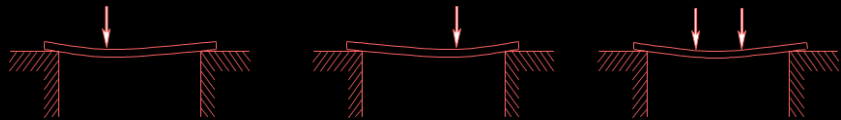


Suvarnabhumi Airport, Bangkok, Thailand





Taut Structures are 'flexible':



(a) a stiff 'structure', such as a bridge, does not change drastically its shape, when loading varies



(b) A 'flexible' structure, such as a cable, can change drastically its shape, when loading varies





Earthquake in Sichuan, China (May, 2008)

Flexible structures must conform to
Funicular shapes:

Those that equilibrate a set of loads, without bending moments



Flexible structures must conform to
Funicular shapes:

Those that equilibrate a set of loads, without bending moments



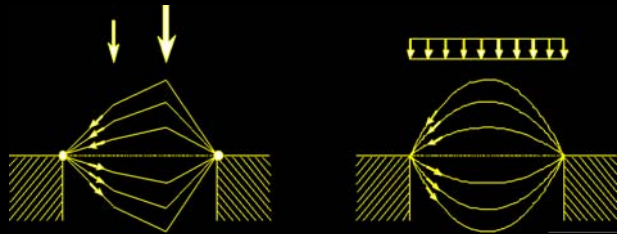
Flexible structures must conform to
Funicular shapes:

Those that equilibrate a set of loads, without bending moments

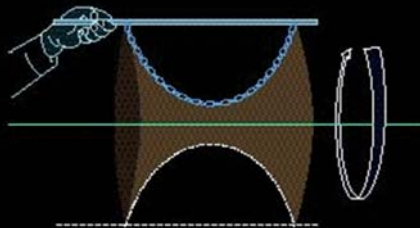




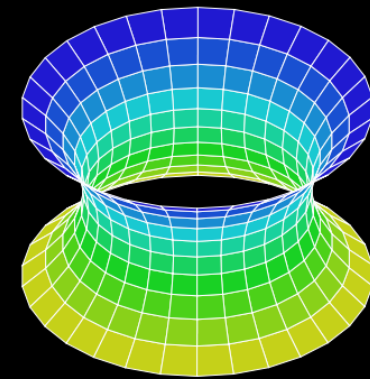
Funicular Shapes:



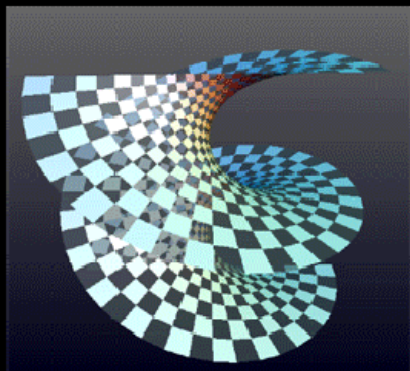
The Catenaria



The Catenoid:



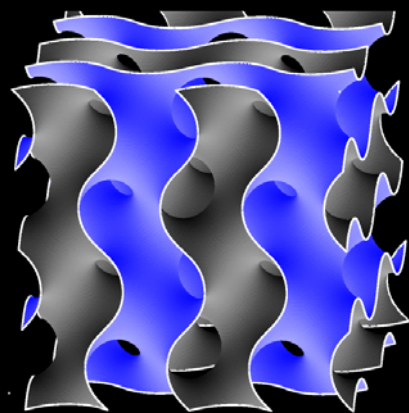
The Helicatenoid



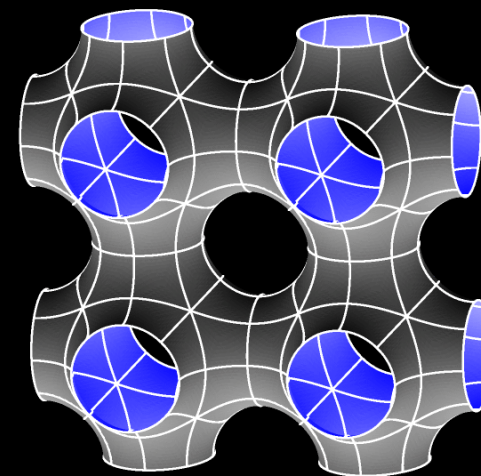
A gyroid (Alan Schoen, 1970)



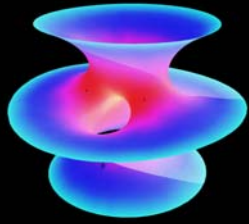
A gyroid (Alan Schoen, 1970)



A Schwarz-P surface



Costa's Surface (1982):



Helaman Ferguson, 1999

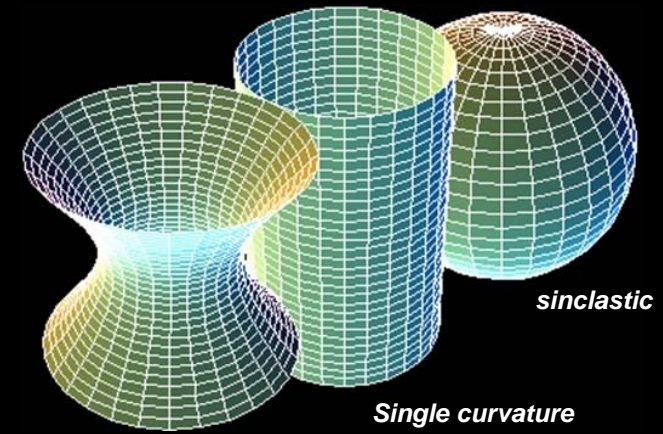


Helaman Ferguson, 2008



AUSTRALIAN WILDLIFE HEALTH CENTRE

Double curvature superfaces

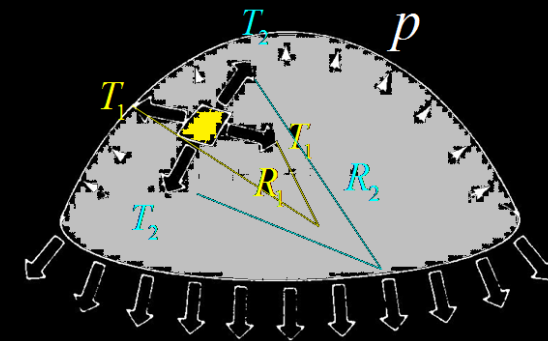


anticlastic

Single curvature

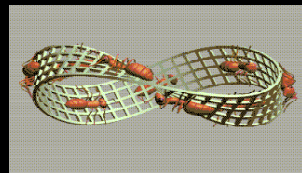
sinclastic

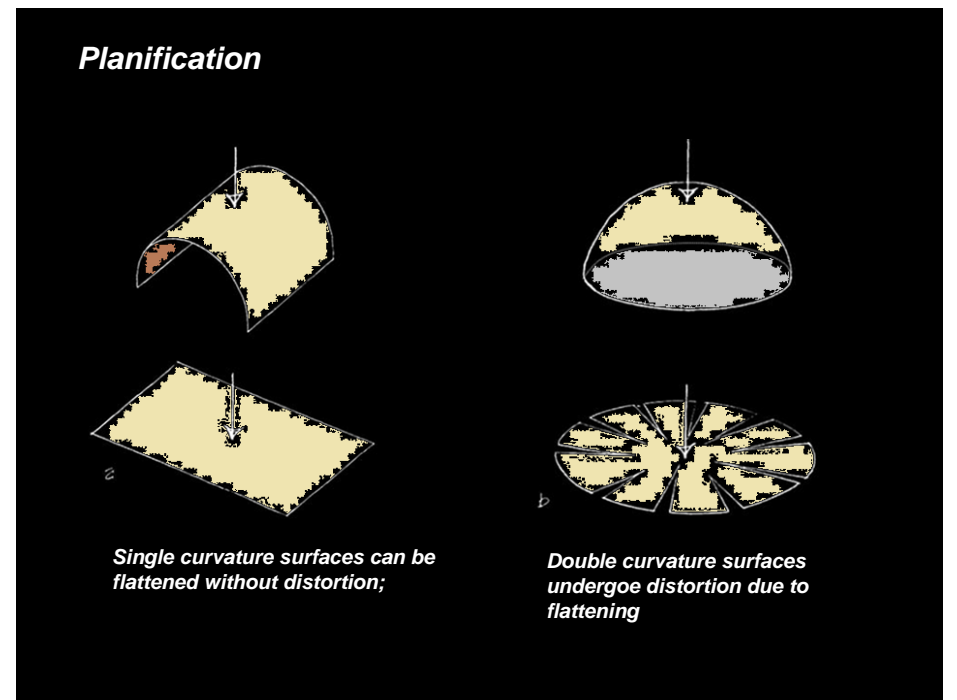
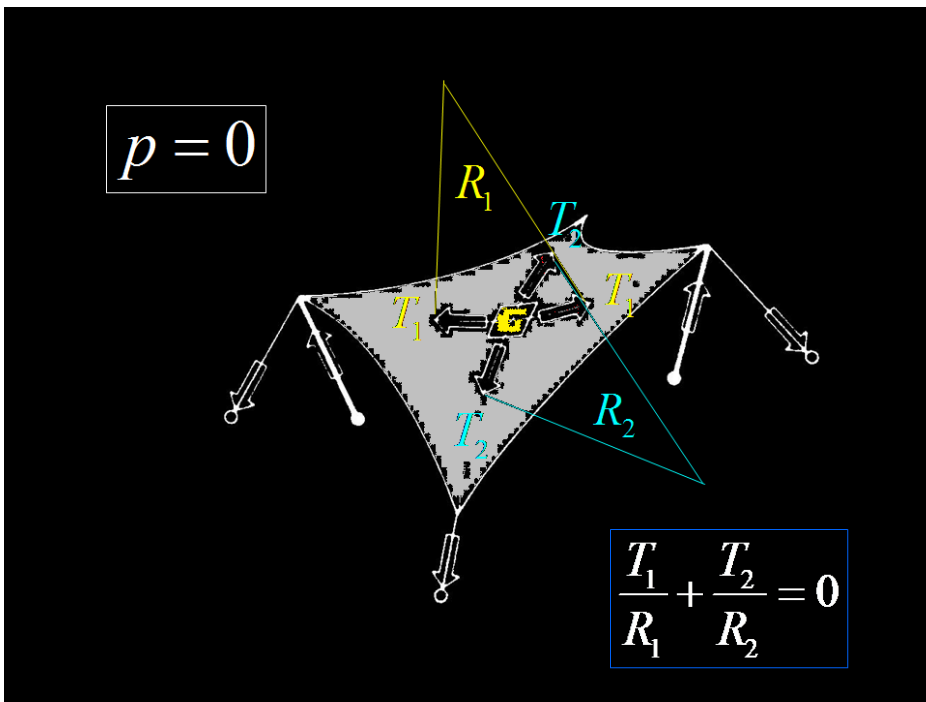
**Equação de Laplace-Young
(equação das bolhas de sabão, ou das membranas):**

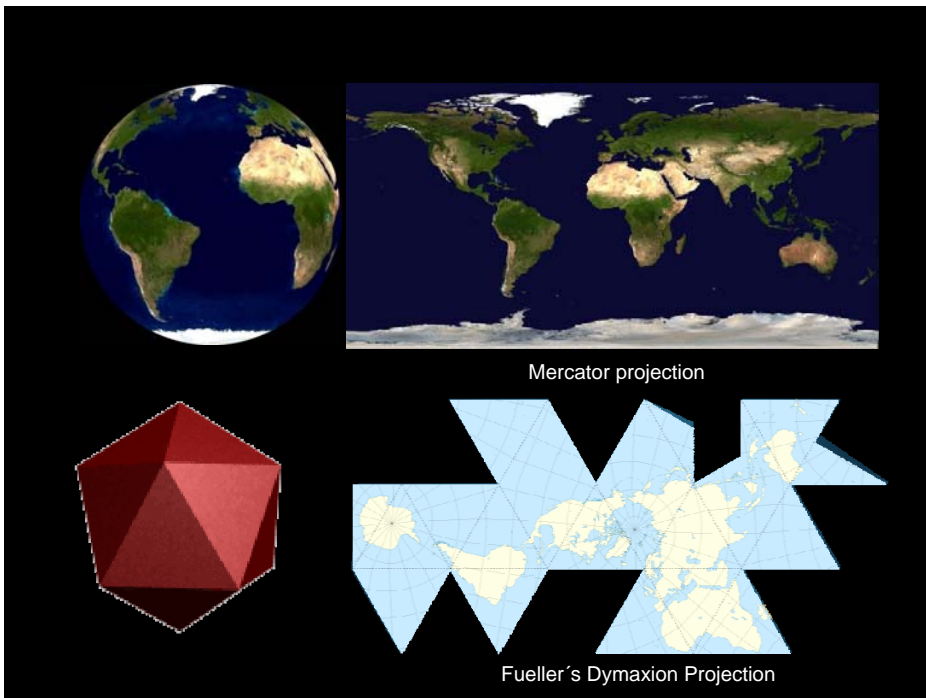
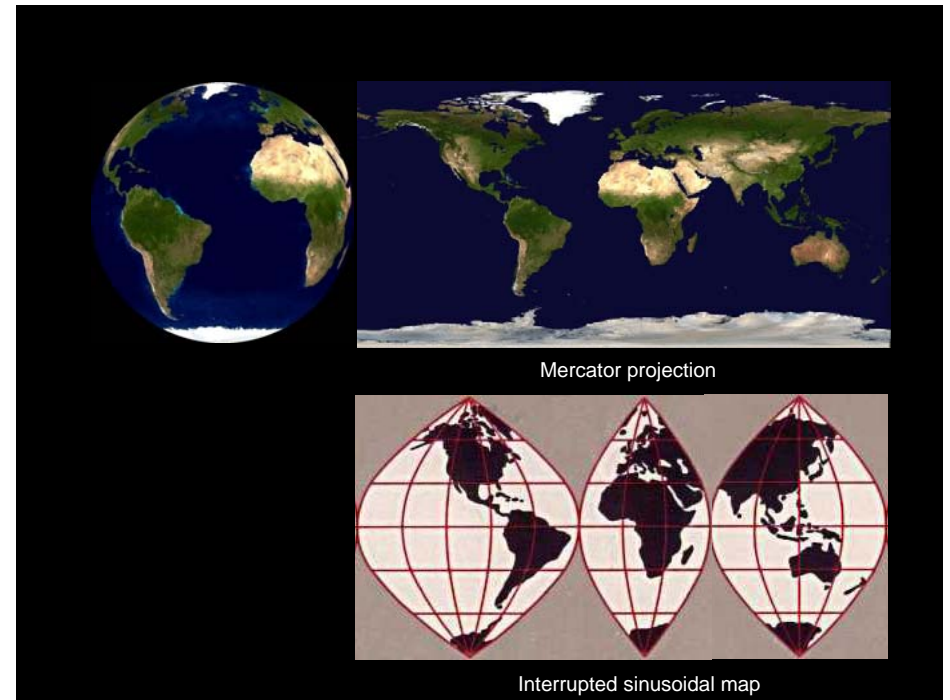
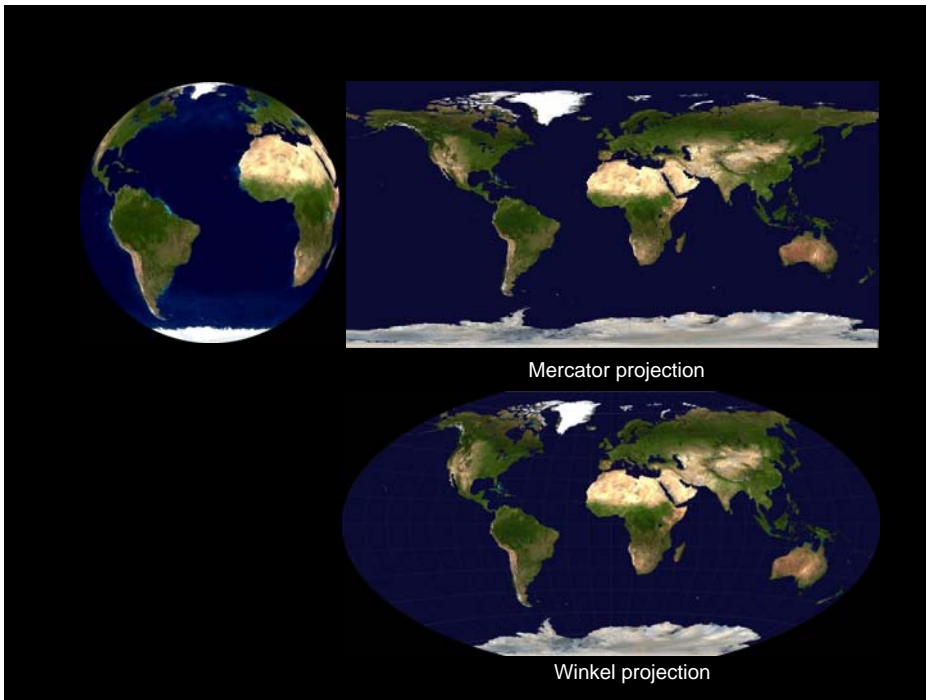


$$\frac{T_1}{R_1} + \frac{T_2}{R_2} = p$$

A triangle immersed in a saddle-shape plane (a hyperbolic paraboloid), as well as two diverging ultraparallel lines.







The Design Process of Taut Structures

"No other class of architectural structural systems is as dependent upon the use of digital computers as are tensile membrane structures".

David Campbel [ASCE Second Civil Engineering Automation Conference, 1991].

ARCHITECTURAL INTENTION:



PROJECT / ANALYSIS:



Initial, non-viable shape



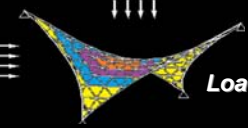
Busca da forma

Final, viable shape

Determinação dos padrões de corte

Resposta aos carregamentos

Patterning and flattening:

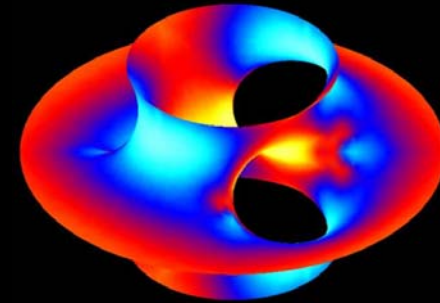


Load analysis

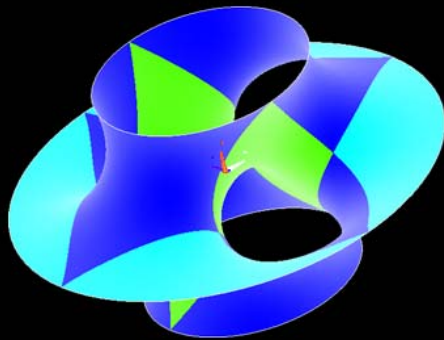
DESIGN SOLUTION:



Costa's Surface:

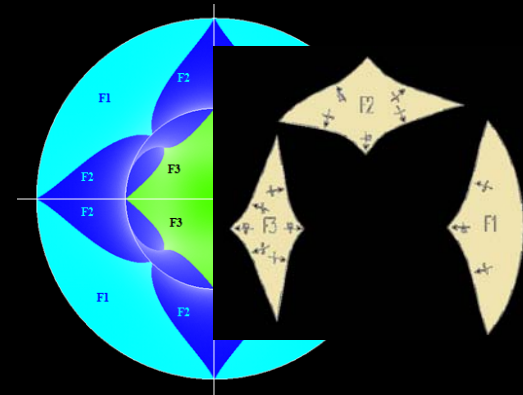


Costa's Surface:



Symmetries & Patterns

Costa's Surface:



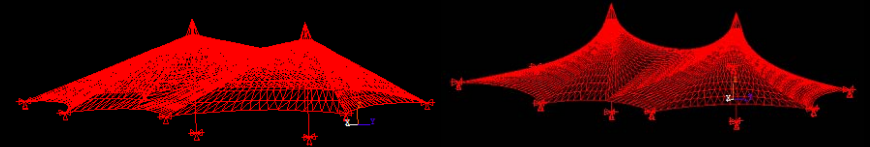
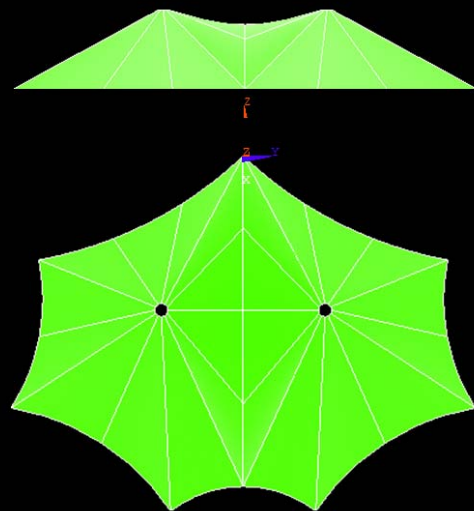
Symmetries & Patterns

Costa's Surface:



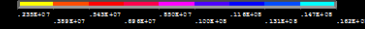
Realization: Lycra sculpture at EPUSP (2008)

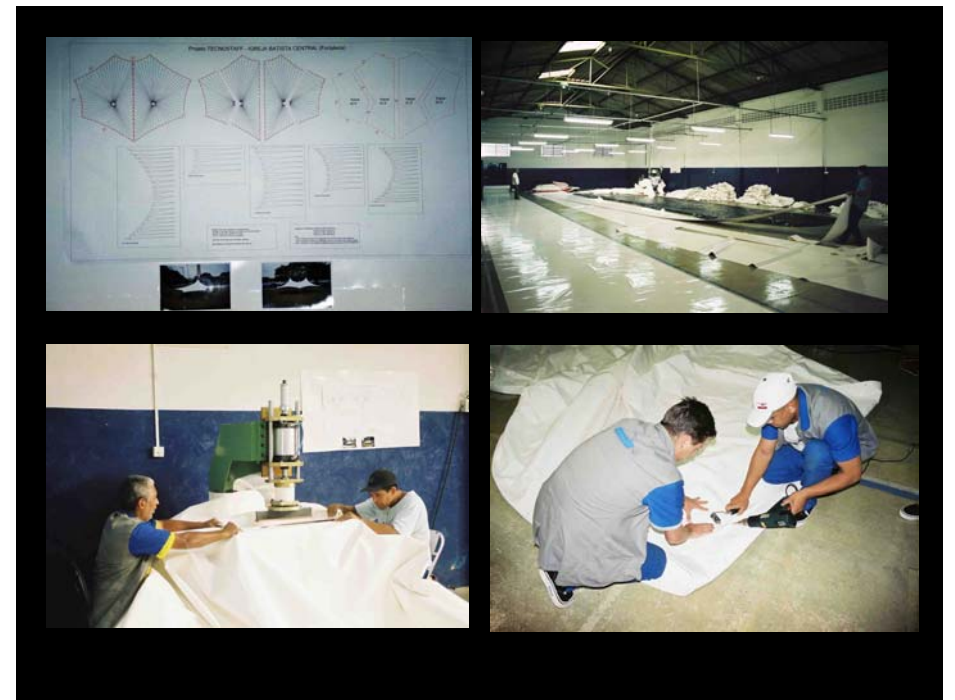
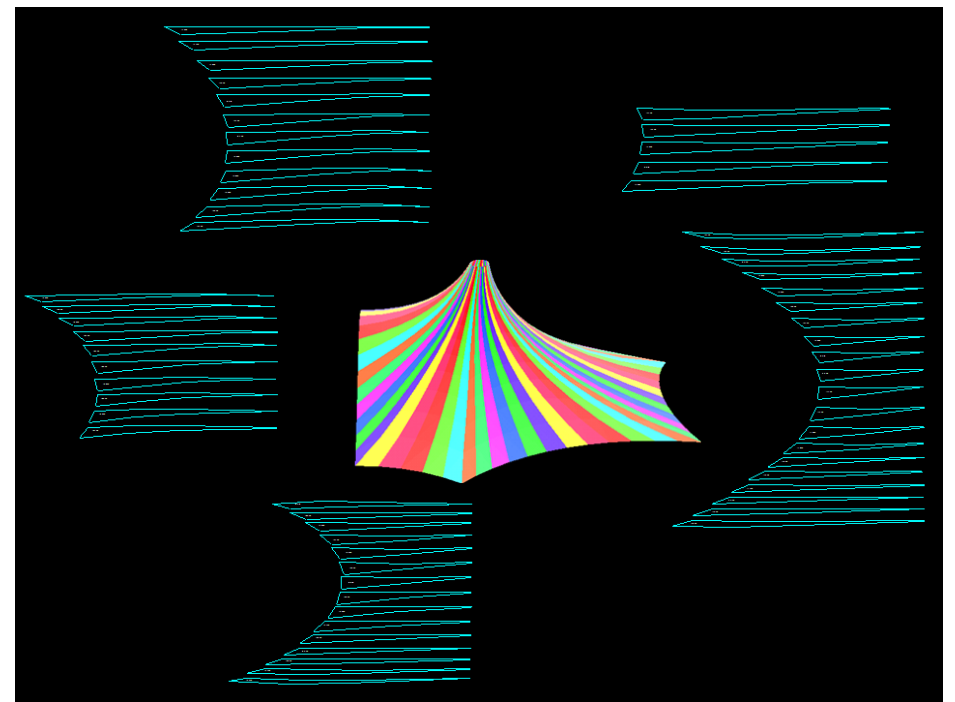
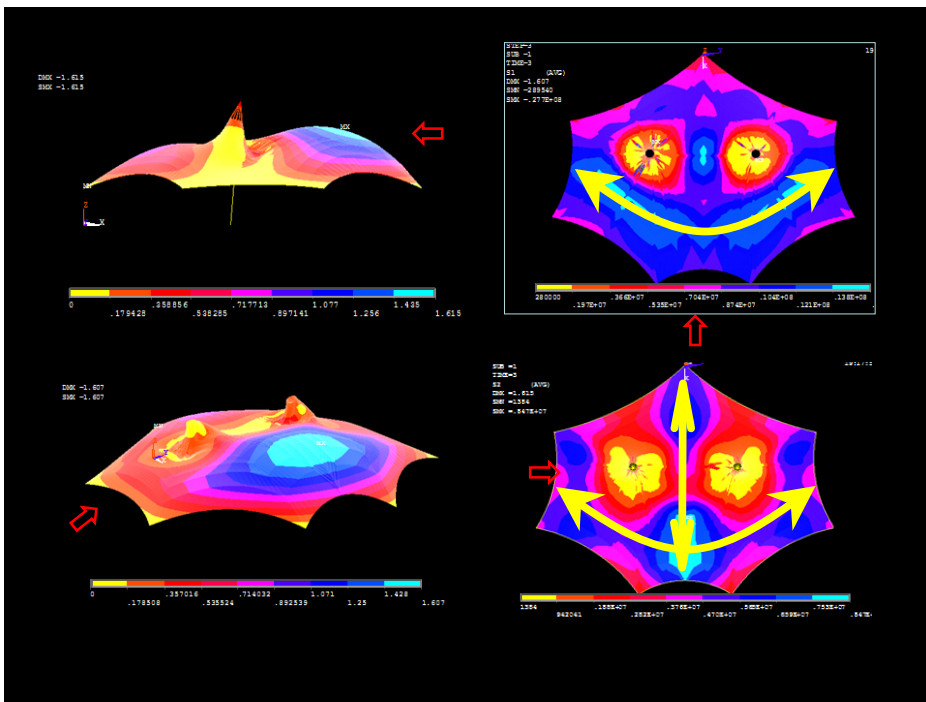
Igreja Batista Central Fortaleza (2003)

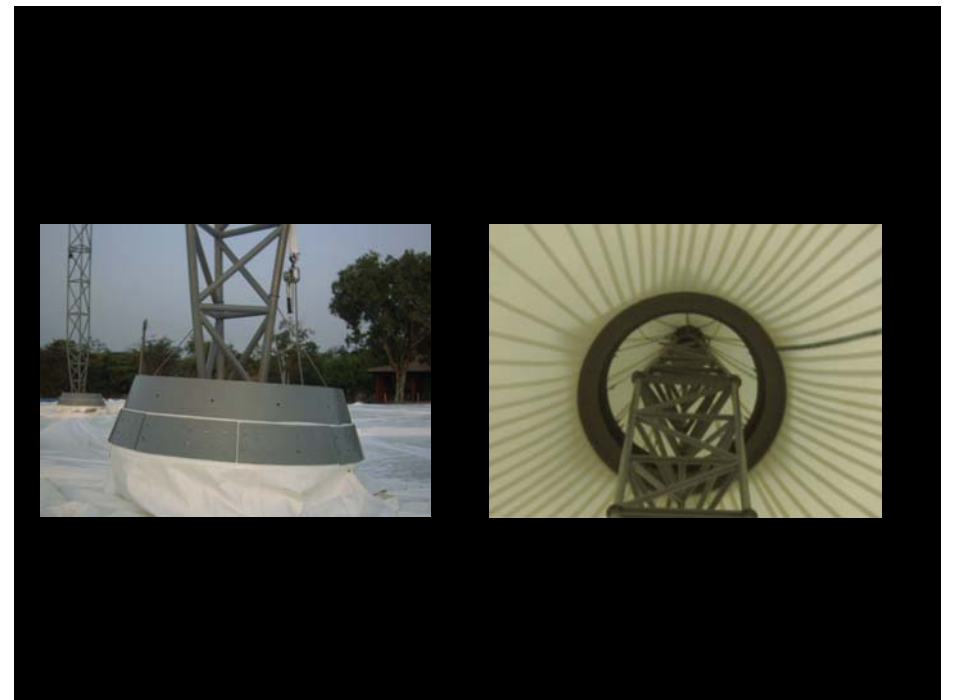


1128902
108 461
1000042
25
(0770)
100 4 241139
100 4 241139
100 4 1228-15

100 27 2028
18 188 008

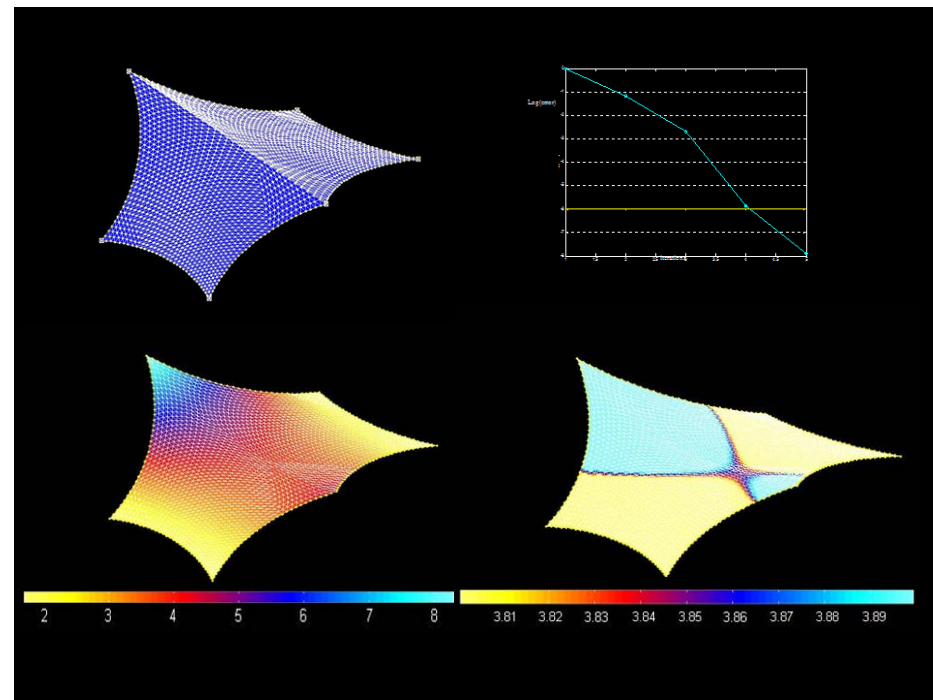






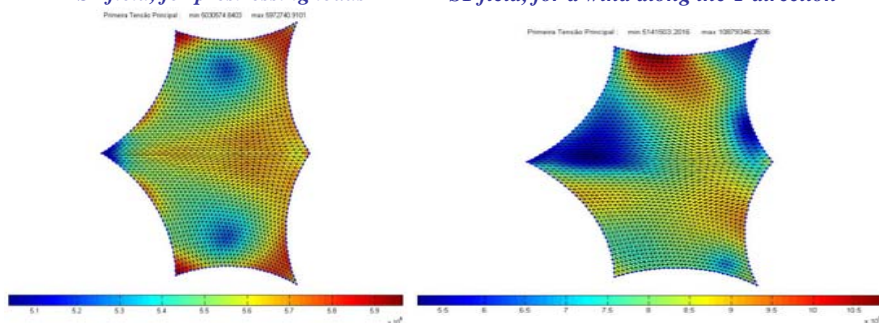


The membrane roof of the "Memorial dos Povos" of Belém do Pará

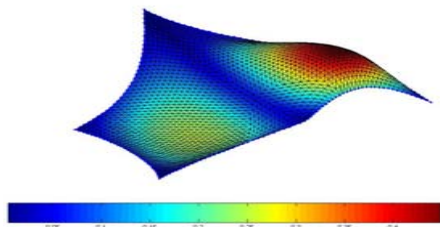


SI field, for prestressing loads

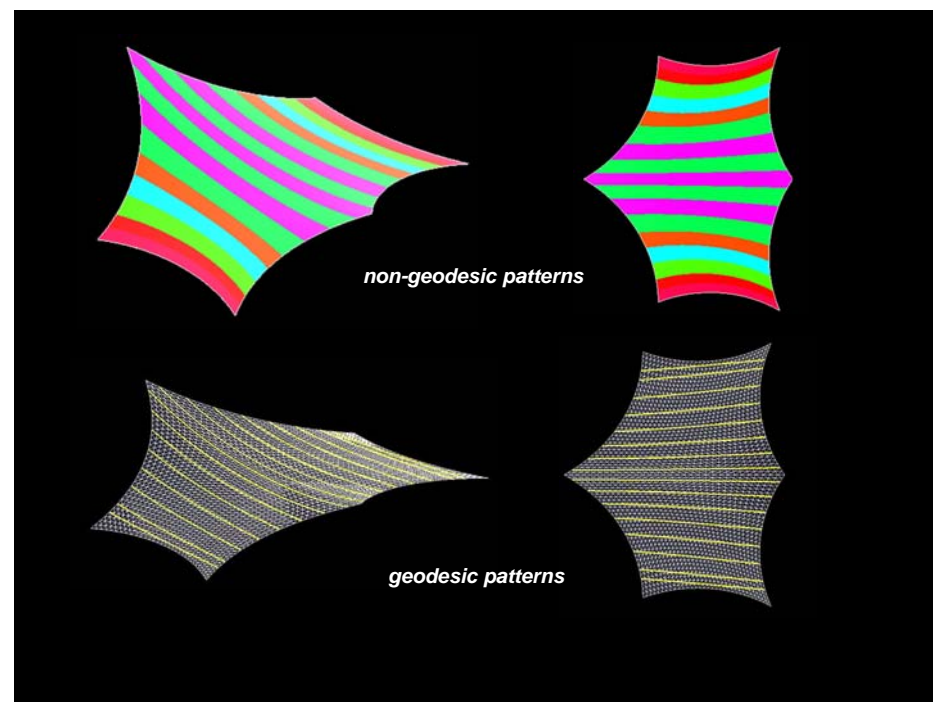
SI field, for a wind along the Y direction

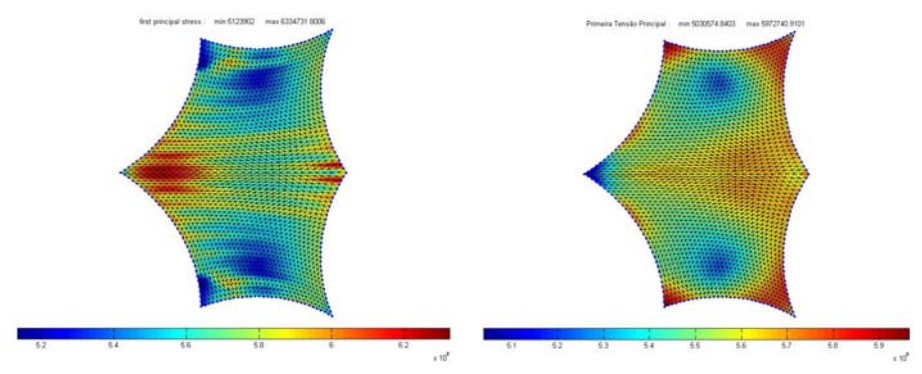
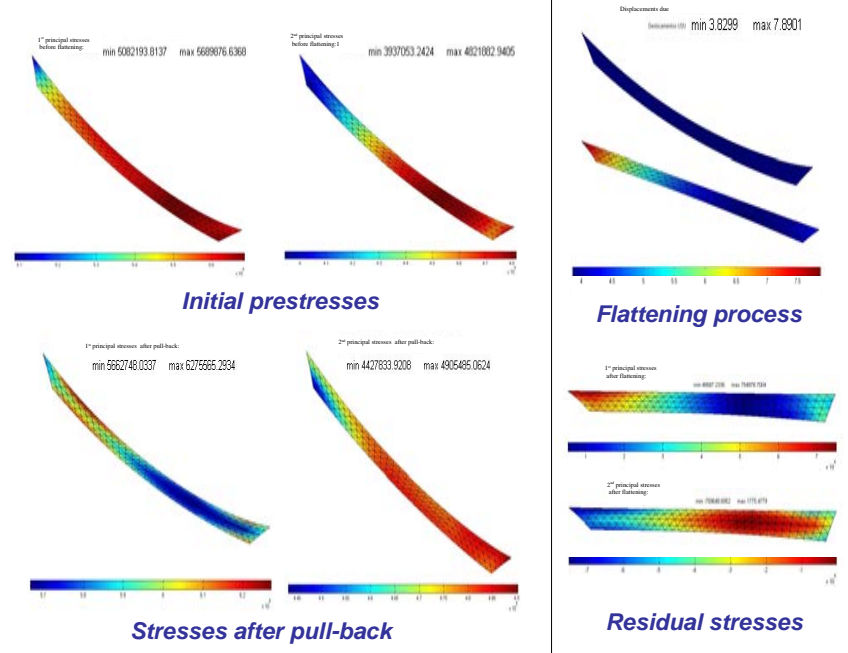
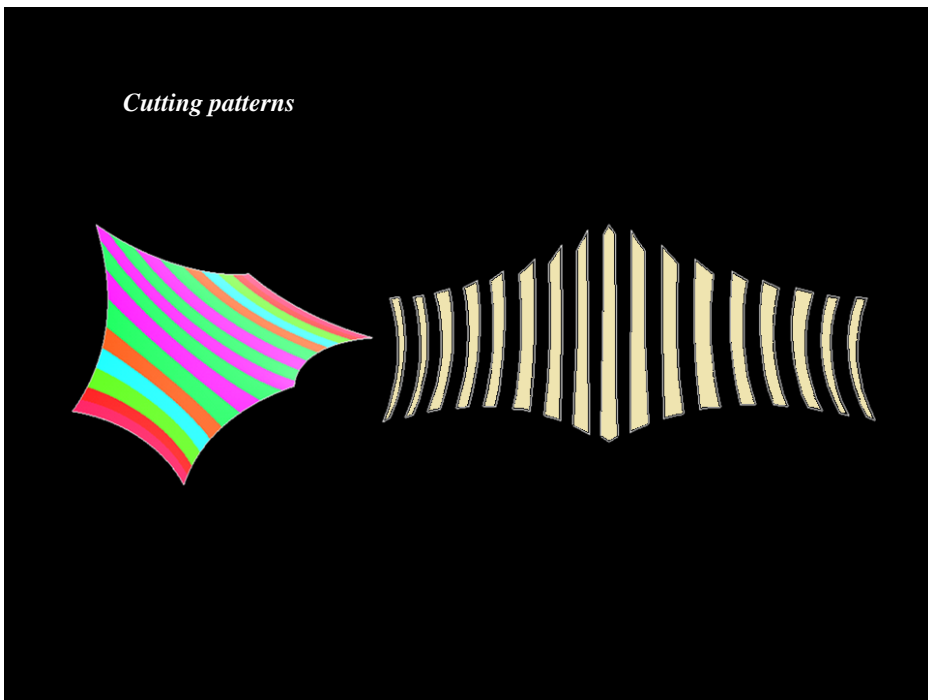


Displacement U22(M) min: 0 max: 0.45206



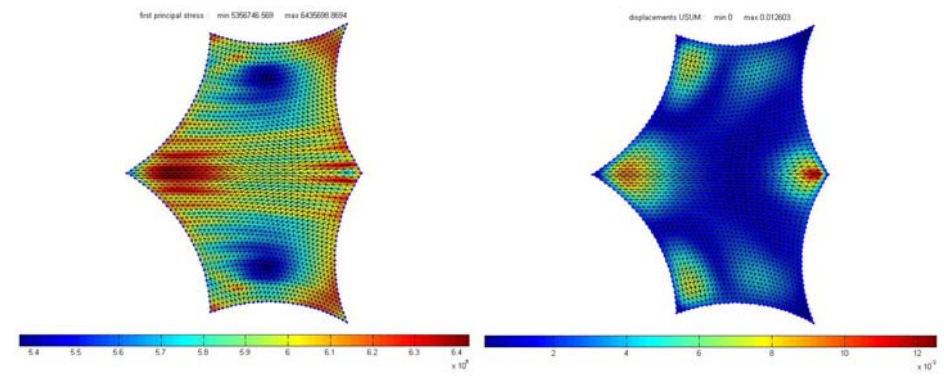
displacement norms, for a wind along the Y direction





Maximum first principal stresses after planification and pull-back

Maximum first principal stresses for the prestress load case, as initially calculated



Maximum first principal stresses after relaxation of pull-back stresses

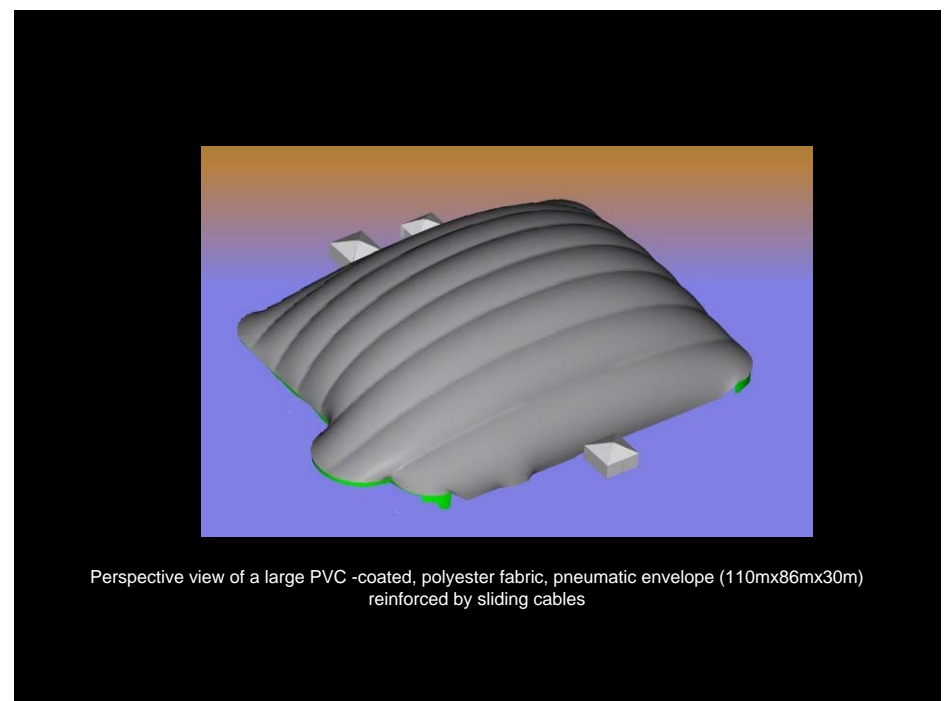
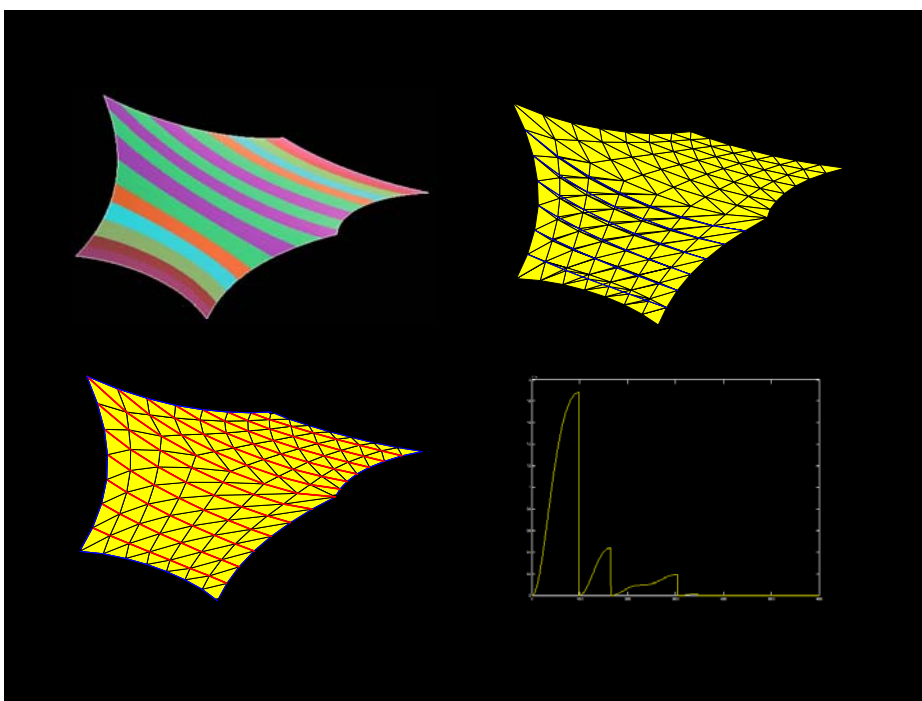
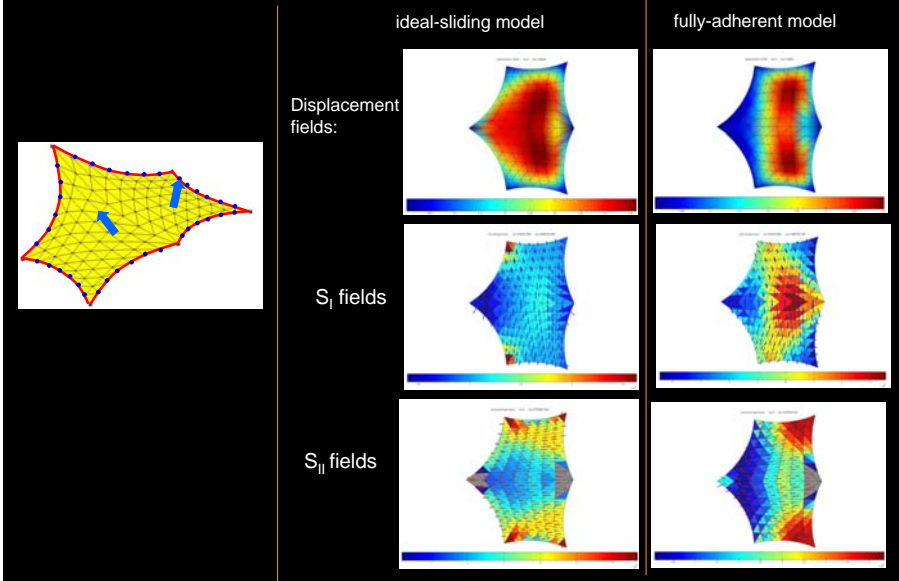
Displacements due to relaxation of pull-back stresses

SLIDING-CABLES

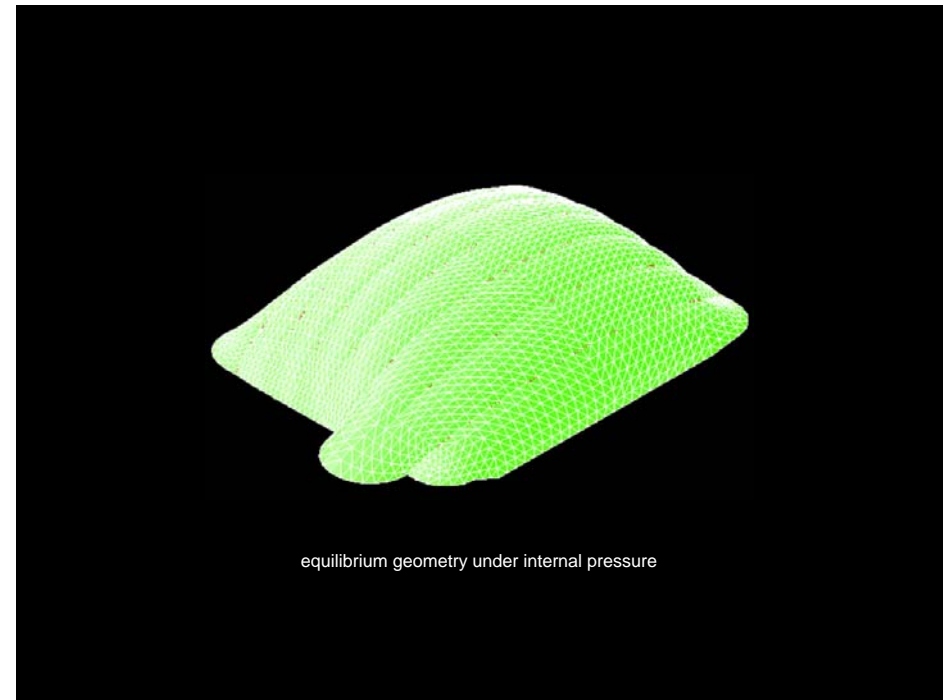
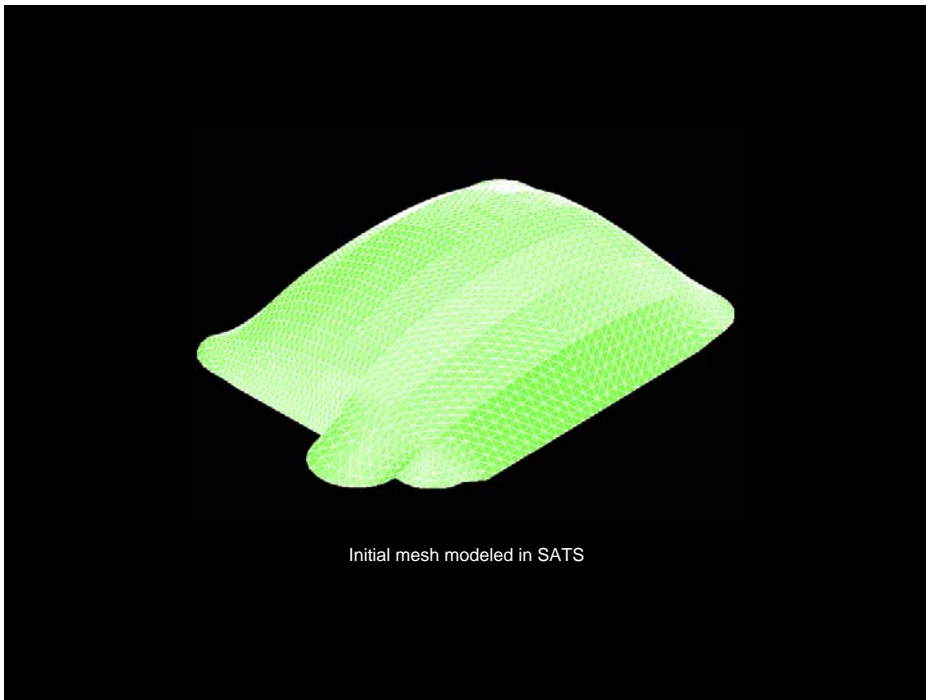


(September 2009)

The Memorial dos Povos de Belém do Pará

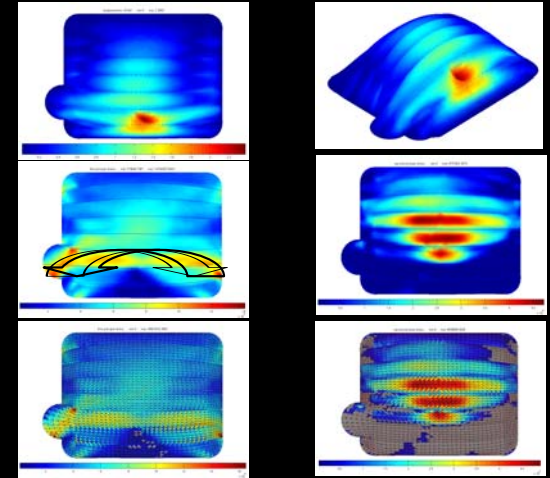
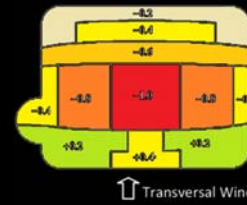


Perspective view of a large PVC-coated, polyester fabric, pneumatic envelope (110mx86mx30m) reinforced by sliding cables



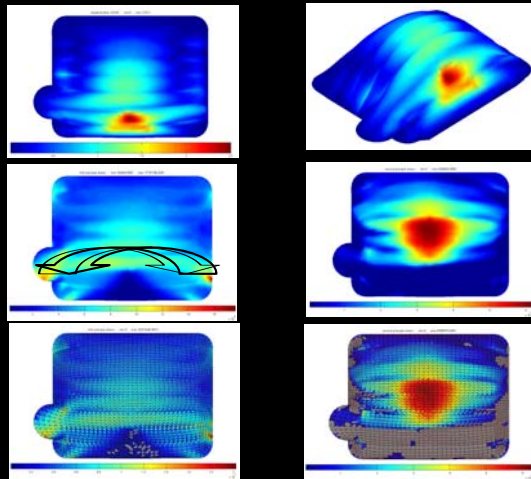


“LC1A” – Transversal wind, **adherent cables**



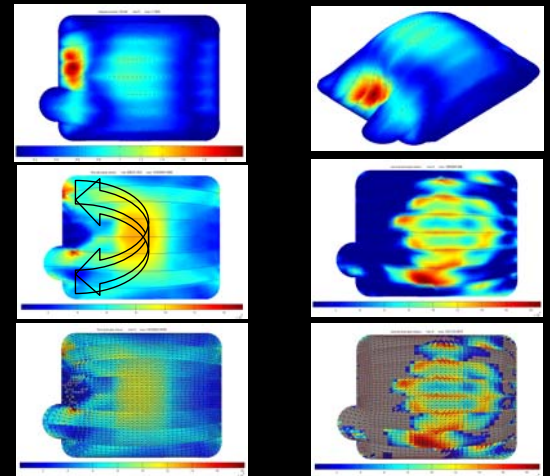
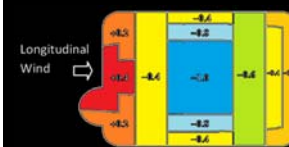
(a) field of displacement norms; (b) *idem*, isometric view; (c) stress field; (d) stress field.

“LC1S” – Transversal wind, **sliding cables**



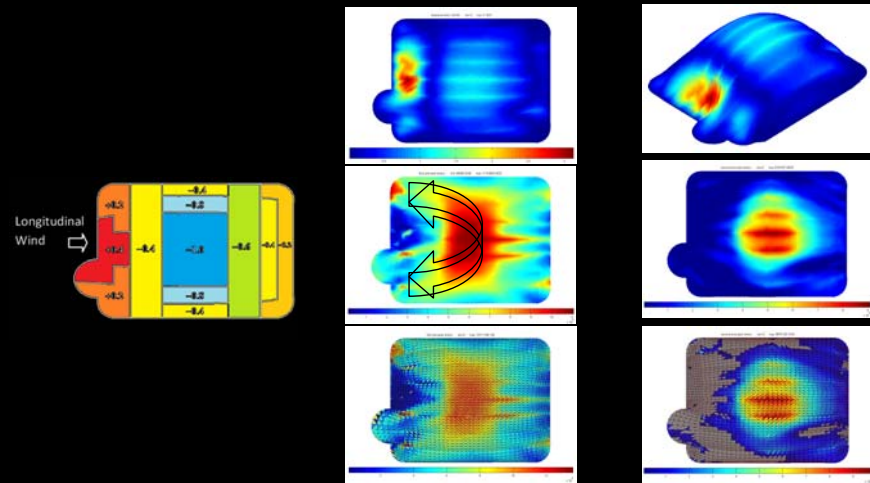
(a) field of displacement norms; (b) *idem*, isometric view; (c) stress field; (d) stress field.

“LC2A” – Longitudinal wind, **adherent cables**



(a) field of displacement norms; (b) *idem*, isometric view; (c) stress field; (d) stress field.

“LC2S” – Longitudinal wind, sliding cables



(a) field of displacement norms; (b) *idem*, isometric view; (c) stress field; (d) stress field.

Table 1. Initial normal loads for the longitudinal cables [kN]

| Cable | 1 | 2 | 3 | 4 | 5 | 6 | 7 |
|-------|-----|----|----|----|----|----|-----|
| N_0 | 100 | 60 | 50 | 40 | 50 | 80 | 100 |

Table 2. Normal loads on the adherent cables [kN]

| Load Case | Cable | $N_{average}$ | N_{max} | N_{min} |
|------------------------------|-------|---------------|-----------|-----------|
| LC0A Internal Pressure | 1 | 107 | 117 | 103 |
| | 2 | 58 | 65 | 41 |
| | 3 | 47 | 50 | 43 |
| | 4 | 40 | 47 | 20 |
| | 5 | 44 | 53 | 27 |
| | 6 | 80 | 120 | 47 |
| | 7 | 101 | 122 | 73 |

| | | | | |
|--|---|-----|-----|-----|
| LCIA Transversal Wind, Adherent Cables | 1 | 198 | 224 | 187 |
| | 2 | 137 | 148 | 108 |
| | 3 | 139 | 157 | 117 |
| | 4 | 130 | 180 | 62 |
| | 5 | 154 | 203 | 117 |
| | 6 | 138 | 214 | 89 |
| | 7 | 46 | 92 | 30 |

| | | | | |
|---|---|-----|-----|-----|
| LC2A Longitudinal Wind, Adherent Cables | 1 | 258 | 290 | 236 |
| | 2 | 137 | 180 | 107 |
| | 3 | 97 | 145 | 43 |
| | 4 | 81 | 136 | 0 |
| | 5 | 100 | 153 | 12 |
| | 6 | 205 | 307 | 131 |
| | 7 | 227 | 310 | 120 |

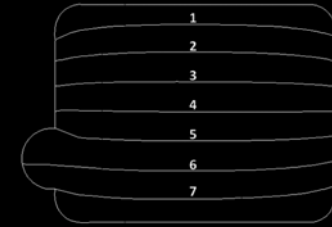
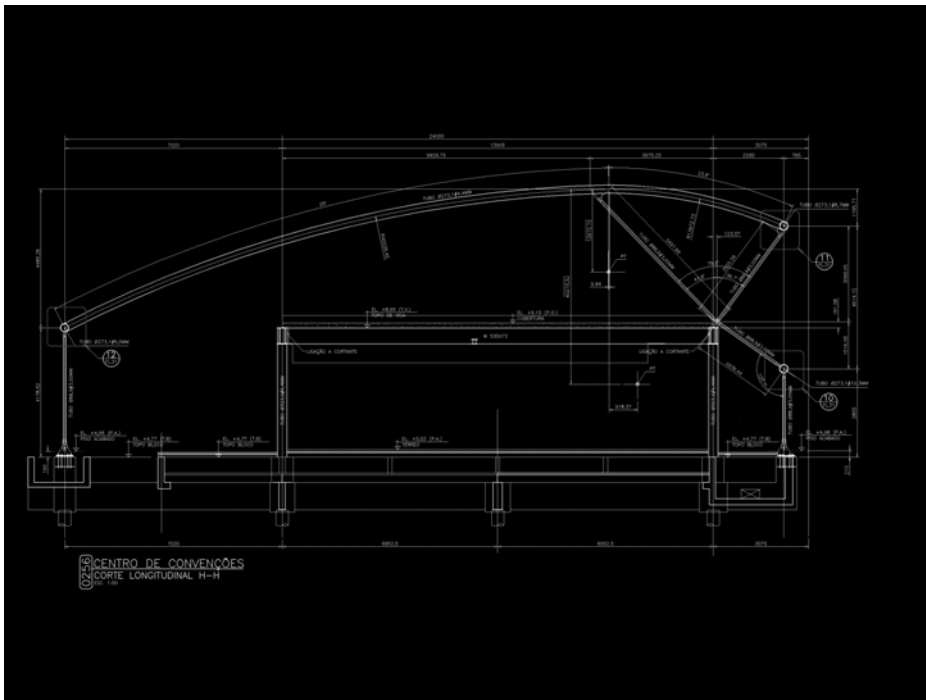


Table 3. Comparison between normal loads on adherent and sliding cables [kN]

| Cable | N_0 | Internal Pressure | | Wind loads | | Longitudinal Wind | |
|-------|-------|-------------------|-------------------|---------------------------------------|-------------------|-------------------|-------------------|
| | | LC0A (average) | LC0S (uniform) | Transversal wind LC1A (average) | LC1S (uniform) | LC2A (average) | LC2S (uniform) |
| 1 | 100 | 107 | 107 | 198 | 195 | 258 | 250 |
| 2 | 60 | 58 | 57 | 137 | 133 | 137 | 128 |
| 3 | 50 | 47 | 47 | 139 | 135 | 97 | 80 |
| 4 | 40 | 40 | 38 | 130 | 124 | 81 | 45 |
| 5 | 50 | 44 | 42 | 154 | 149 | 100 | 61 |
| 6 | 80 | 80 | 70 | 138 | 123 | 205 | 184 |
| 7 | 100 | 101 | 100 | 46 | 45 | 227 | 217 |





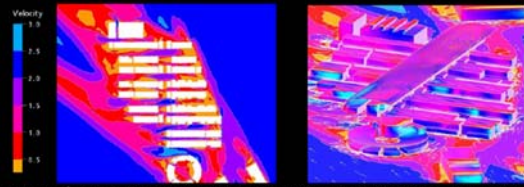


Figura 4 – À esquerda, distribuição da velocidade do vento no nível do pedestre, a 1,5m. Observar escala de velocidades de 0m/s a 3m/s. À direita, distribuição de pressões de vento sobre as envoltórias.

